PLOS ONE

RESEARCH ARTICLE

Mutations close to a hub residue affect the distant active site of a GH1 β-glucosidase

Valquiria P. Souza, Cecília M. Ikegami, Guilherme M. Arantes, Sandro R. Marana*

Departamento de Bioquímica, Instituto de Química, Universidade de São Paulo, São Paulo, SP, Brazil

* srmarana@iq.usp.br

OPEN ACCESS

Citation: Souza VP, Ikegami CM, Arantes GM, Marana SR (2018) Mutations close to a hub residue affect the distant active site of a GH1 β-glucosidase. PLoS ONE 13(6): e0198696. https://doi.org/10.1371/journal.pone.0198696

Editor: Andreas Hofmann, Griffith University, AUSTRALIA

Received: March 5, 2018

Accepted: May 23, 2018

Published: June 6, 2018

Data Availability Statement: All relevant data are within the paper and supporting figures.

Funding: This project was supported by FAPESP (Fundação de Amparo à Pesquisa do Estado de São Paulo; Grants 08/57619-4, 14/19439-5 and 16/22365-9) to Sandro R. Marana and Valquiria P Souza, CNPq (Conselho Nacional de Desenvolvimento Científico e Tecnológico) to Guilherme Menegon Arantes and Sandro R. Marana, and CAPES (Coordenação de Aperfeiçoamento de Pessoal de Nível Superior) to Cecilia Midori Ikegami and Sandro R. Marana. The

Abstract

The tertiary structure of proteins has been represented as a network, in which residues are nodes and their contacts are edges. Protein structure networks contain residues, called hubs or central, which are essential to form short connection pathways between any pair of nodes. Hence hub residues may effectively spread structural perturbations through the protein. To test whether modifications nearby to hub residues could affect the enzyme active site, mutations were introduced in the β-glycosidase Sfβgly (PDB-ID: 5CG0) directed to residues that form an α-helix (260–265) and a β-strand (335–337) close to one of its main hub residues, F251, which is approximately 14 Å from the Sfβgly active site. Replacement of residues A263 and A264, which side-chains project from the α-helix towards F251, decreased the rate of substrate hydrolysis. Mutation A263F was shown to weaken noncovalent interactions involved in transition state stabilization within the Sfβgly active site. Mutations placed on the opposite side of the same α-helix did not show these effects. Consistently, replacement of V336, which side-chain protrudes from a β-strand face towards F251, inactivated Sfβgly. Next to V336, mutation S337F also caused a decrease in noncovalent interactions involved in transition state stabilization. Therefore, we suggest that mutations A263F, A264F, V336F and S337F may directly perturb the position of the hub F251, which could propagate these perturbations into the Sfβgly active site through short connection pathways along the protein network.

Introduction

The Protein Structure Network (PSN) is an interesting tool for analysis of the tertiary structure of proteins [1]. The approach permits a global analysis of the complete set of noncovalent interactions in the protein structure, resulting in a compact view of the role of each residue within the structure network. PSN representations improve the analysis of specific residues and their interactions, avoiding biased choices among the myriad of contact sets that can be built from the protein structure [1].

PSNs have "small-world" properties, exhibiting high local connectivity, a high clustering coefficient (C) and a small average shortest contact pathway (L, also known as path length). A small number of contacts (usually around 3 to 5) is enough to link any two protein residues, even those distant through structure [2–7].

funders had no role in study design, data collection and analysis, decision to publish, or preparation of the manuscript.

Competing interests: The authors have declared that no competing interests exist.

Abbreviations: NPβfuc, *p*-nitrophenyl β-fucoside; NPβgal, *p*-nitrophenyl β-galactoside; NPβglc, *p*-nitrophenyl β-glucoside; PSN, Protein Structure Network; Sfβgly, β-glucosidase from *Spodoptera frugiperda*.

Two centrality parameters calculated from the PSN are useful to characterize the relative importance of individual residues in establishing short contact pathways: betweenness centrality is the frequency a given residue is among the shortest contact pathways through the protein structure; closeness centrality presents the average number of contacts one residue performs with the remaining protein. Residue centrality can also be evaluated by the increase in path length when a specific residue is removed from the PSN [6].

The PSN approach has revealed that core residues in enzyme active sites [8] and allosteric pathways [9–14] have high closeness centrality. Point mutations directed to the same contact pathway have an additive effect [15; 16], whereas mutations directed to residues connecting to the same active site region, exhibit coherent qualitative effects on enzyme activity [17]. These observations suggest that central residues of the PSN may indicate regions or residues which spread perturbations more easily along the protein structure. Thus, measures of residue centrality could also be combined with structural analysis to help identifying residues involved with the protein function.

Sfβgly is a GH1 β-glucosidase from the fall armyworm *Spodoptera frugiperda* that has a (β/α) 8 barrel fold and an active site composed of 4 subsites (-1, +1, +2 and +3) located in a pocket at the top of the central barrel (PDB ID: 5CG0) [18; 17]. Sfβgly catalyzes the hydrolysis of *p*-nitrophenyl β-glycosides and oligocellodextrins [18] using a double-displacement mechanism in which E187 is the catalytic acid and E399 is the catalytic nucleophile [19; 20]. Subsite +1, closer to the active site entrance, is formed by residues W371, E190, E194 and K201. The contribution of the latter three residues to the specificity of binding the substrate aglycone has been previously characterized [21]. Subsite -1, located in the bottom of the active site pocket, interacts with the substrate glycone, which may be glucose, galactose or fucose. Residues Q39 and E451 are essential to the subsite -1 specificity for the substrate glycone due to hydrogen bonds with the hydroxyl groups 4 and 6 of the monosaccharidic glycone [22–24].

The PSN of Sfβgly has "small-world" properties and presents 11 hub residues (R97, F251, S358, E399, T245, K366, F334, S247, N249, Y420 and Y331) identified by their relevance to the shortest path length [25] (S1 Table). Removal of these residues from the PSN resulted in path length increments significantly higher than the average increament (S1 Table) [25]. Among these hub residues, F251 is the highest ranked among the eight hubs (F251, S358, T245, K366, F334, S247, N249 and Y420) placed outside of the active site (S1 Table). Removal of F251 from the PSN increases the path length in 6 standard deviations. Consistently, experiments have shown that point mutantions directed towards hub residues as well as towards residues surrounding F251 decreased thermal stability of Sfβgly [25].

Here we analyze the effect on Sfβgly enzymatic activity of mutations in the region surrounding F251, which is approximately 14 Å distant from the active site (the catalytic nucleophile E399 was taken as reference point for the active site). Effects of mutations were probed by determining steady-state kinetic parameters for substrate hydrolysis (*p*-nitrophenyl β-glycosides and cellobiose) and, based on them, the stability of the enzyme-transition state ($ES^{\ddagger}$) complex. Therefore, we evaluated how effectively mutations around a PSN hub affect a distant active site.

Materials and methods

Expression and purification of the wild-type and mutant Sfβgly

The pET46 vectors (Merck Millipore; Billerica, MA, USA) encoding for the wild-type and mutant Sfβgly were previously described [25]. Recombinant enzymes were produced in Nova-Blue (DE3) bacteria using the previously described protocol [25]. The enzyme purification was performed using nickel-nitrilotriacetic acid resin (Qiagen, Valencia, CA, USA) [25]. Samples of the purified enzymes were submitted to buffer exchange using HiTrap desalting columns

(GE HealthCare, Little Chalfont, UK) following the manufacturer instructions. Circular dichroism and tryptophan fluorescence spectra were employed to check the proper folding of the purified enzymes [25]. The protein concentrations were determined from the absorbance at 280 nm in the presence of 6 M guanidium hydrochloride prepared in 50 mM sodium phosphate at pH 6.5. The extinction coefficients of the wild-type and mutant proteins were calculated as previously described [26; 27].

Enzyme kinetic analysis

The initial rates for the hydrolysis of the *p*-nitrophenyl β-glycosides (NPβglc, *p*-nitrophenyl β-glucoside; NPβgal, *p*-nitrophenyl β-galactoside; NPβfuc, *p*-nitrophenyl β-fucoside) and cellobiose were determined at 30˚C using substrates prepared in 50 mM sodium citrate–sodium phosphate buffer at pH 6. The hydrolysis of the *p*-nitrophenyl β-glycoside substrates was detected by following the production of *p*-nitrophenolate, whereas hydrolysis of cellobiose was detected by the glucose production. The production of two glucoses from one cellobiose was taken into account in the calculations. At least ten substrate concentrations, bracketing the K_m values, were used for the determination of the enzyme kinetic parameters (K_m and k_{cat}). Rate and substrate concentration data were fitted to the Michaelis-Menten equation using the Origin 2017 software, version b9.4.0.220 (Origin Lab, Northampton, MA, USA).

Determination of the mutational effect on the stability of the ES‡ complex

The effects of the mutations on the stability of the ES‡ complex were determined using the equation $\Delta\Delta G^{\ddagger} = RT\ln(k_{cat}/K_{m1} / k_{cat}/K_{m2})$, where k_{cat}/K_m were determined for the hydrolysis of the same substrate by the mutant (1) or wild-type (2) enzyme [28; 29]. T is 303 K. The hydrolytic reaction catalyzed by β-glucosidases is divided in two steps, glycosylation and deglycosylation, each of them has an ES‡ complex, as represented in the S1 Fig [19; 29]. In that scheme $k_{cat}/K_m = (k_1k_2) / (k_2 + k_{-1})$, corresponding to the rate constant for the glycosylation step (S1 Fig). Free energy changes ($\Delta G^{\ddagger}$) calculated with this parameter relate to differences between glycosylation ES‡ and free enzyme and substrate. Assuming that wild-type and mutant enzymes present similar ground states, $\Delta\Delta G^{\ddagger}$ indicates differences between two ES‡ [29]. A $\Delta\Delta G^{\ddagger}$ higher than 3 kJ/mol was considered to be significant because this is the lower limit for destabilization of the ES‡ complex due to the disruption of one hydrogen bond [30].

Results and discussion

The PSN hub residues may effectively spread mutational perturbations through the protein structure. For instance, in the specific case of the β-glycosidase Sfβgly, mutations that perturb the environment near the PSN hub F251 reduced its thermostability [25]. To evaluate the hypothesis that PSN hub residues could influence the functional properties of enzymes, here we investigate whether the mutational perturbation spreading from the hub F251 is propagated into the Sfβgly active site, altering its catalytic properties. F251 is part of a group of hub residues (T245, S247, N249 and F251) that extends from the surface to the Sfβgly core [25] and places F251 at a short contact distance to the whole Sfβgly structure (Fig 1A). Indeed, the closeness centrality of F251 indicates that at most five contacts are necessary to link it to any residue in the Sfβgly PSN.

In the region closely surrounding F251, we found residues D260, E261, M262, A263, A264 and E265, which are part of an α-helix, and residues L335, V336 and S337, forming a β-strand (Fig 1A). The mutations analyzed in this study, D260A, E261A, M262F, A263F, A264F, E265A, L335A, V336F and S337F, introduced voids (replacements by A) or extra volume (replacements by F) in the vicinity of the central residue F251, potentially perturbing its spatial position and interactions.

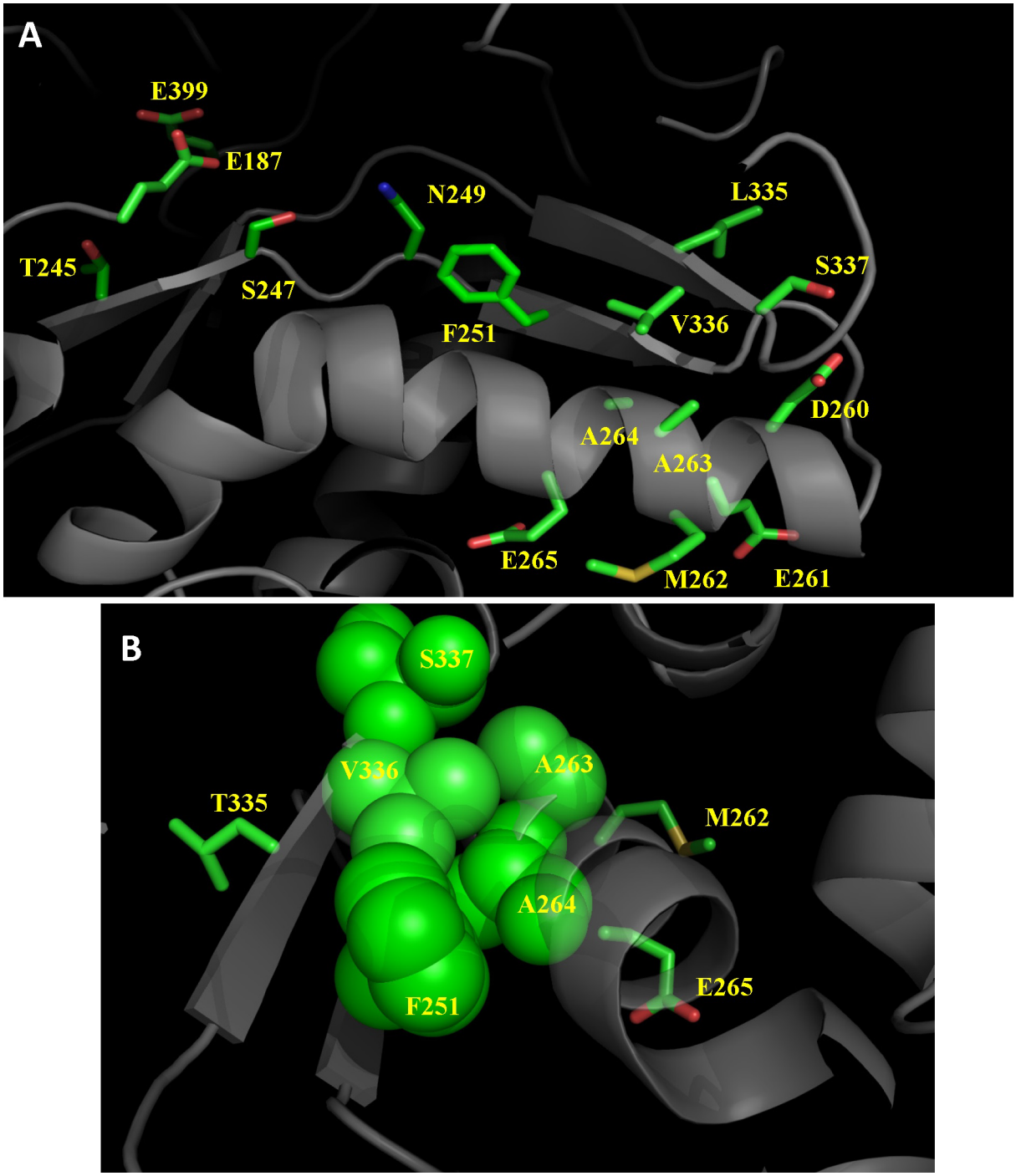

Fig 1. Relative structural positioning of the hub residues, mutated residues and the active site of Sfβgly (5CG0; [17]). Residues D260 to E265 and L335 to S337, which are close to the hub residue F251, were submitted to site-directed mutagenesis. F251, N249, S247 and T245 are hub residues. E187 and E399 are the catalytic acid and nucleophile, respectively. For clarity, only the side chains are shown, some secondary elements were removed and panels A and B are shown in different perspectives. **A**–The hub residues F251, N249, S247 and T245 form a pathway connecting the mutation sites near the protein surface to the core and active site of Sfβgly. The shortest distances are: $F251_{C\varepsilon}$ –$N249_{C\beta}$: 4.1 Å; N249Nδ2 –$S247_{O\lambda}$: 3.9 Å; $S247_{C\beta}$-$T245_{C\beta}$: 7.7 Å; $F251_{C\beta}$ –$A264_{C\beta}$: 5.3 Å; $A264_{C\beta}$ - $A263_{C\beta}$: 5.3 Å. These contacts, except those involving T245, are within the distance limits for noncovalent interactions (*i.e.*, 5 Å). **B**–A different perspective of the mutated residues A263, A264, V336 and S337, which are close to the hub residue F251. The side chains are shown as spheres highlighting the clustering of A263, A264, V336, S337 and F251. The contact distances are near to the upper limit (5 Å) for non-covalent interactions ($F251_{C\beta}$ –$V336_{C\lambda}$: 4 Å; $F251_{C\beta}$ –$A264_{C\beta}$: 5.3 Å; $A264_{C\beta}$ –$A263_{C\beta}$: 5.3 Å). Residues M262, E265 and T335, sites of innocuous mutations, do not take part of this cluster.

https://doi.org/10.1371/journal.pone.0198696.g001

Two mutants, L389A and N391A, were also studied as controls. Residues L389 and N391 are also near to a phenylanaline residue, F280. Moreover, none of these three residues (F280, L389 and N391) are hubs.

Wild-type and mutant Sfβgly were produced in the bacteria NovaBlue (DE3) and purified as previously described [25]. Circular dichroism and tryptophan fluorescence spectra confirmed their correct folding [25]. Steady state kinetic parameters for the hydrolysis of four different substrates (NPβglc, NPβfuc, NPβgal and cellobiose) were determined, except for A264F and V336F (Table 1; S2 Fig). These two mutants showed very low enzyme activity and thermal stability [25], preventing further analysis.

In order to determine the modifications within the Sfβgly active site that altered kinetic parameters (Table 1), the k_{cat}/K_m ratio was used to quantify changes of activation free energy, $\Delta\Delta G^{\ddagger}$ [28; 29] (Table 2; Fig 2). The relative values $\Delta\Delta G^{\ddagger}$ based on the k_{cat}/K_m may represent the stability difference in free energy between two $ES^{\ddagger}$ complexes formed by the wild-type and mutant enzyme (see also the Material and Methods). Thus, this free energy difference probes the mutational effect on interactions involving active site residues and the transition state substrate. Only a $\Delta\Delta G^{\ddagger}$ higher than 3 kJ/mol was considered to be significant because this is the lower limit for destabilization of the $ES^{\ddagger}$ complex due to the disruption of only one hydrogen bond [30].

Using this criteria, only mutations A263F and S337F caused significant changes in $\Delta\Delta G^{\ddagger}$ for the reactions involving substrates NPβglc and cellobiose (Table 2; Fig 2). Replacement of residues D260, E261, M262, E265 and L335, which are part of the same α-helix and β-strand (Fig 1), did not substantially affected the $ES^{\ddagger}$ complex stability. Moreover, L389A, and N391A control mutations, directed to a "non-hub" residue, did not change the Sfβgly kinetic parameters (Table 1) or activation free energy (Fig 2). Hence, A263F and S337F mutations, distant from the active site, altered the noncovalent interactions involved in transition state stabilization. Note that $A263_{C\beta}$ and $S337_{O\gamma}$ are 25 Å away from the catalytic nucleophile $E399_{O\varepsilon}$.

In Sfβgly, the active site residue E451 forms two hydrogen bonds with the 4 and 6 hydroxyl groups of the substrate glycone (OH4 and OH6 hereafter), whereas Q39 forms a hydrogen bond with OH4 (S3 Fig). Hence, they contribute to the catalysis through the stabilization of the $ES^{\ddagger}$ complex [22; 24]. Residues Q39 and E451 and their interactions with $S^{\ddagger}$ are highly conserved among GH1 β-glucosidases, which shows their essential role in the catalytic activity and substrate specificity of those enzymes [31; 32]. Contributions of these noncovalent interactions to transition state stabilization were previously determined based on comparison of k_{cat}/K_m for Sfβgly wild-type and mutants lacking the side chains of residues 39 and 451, Q39A and E451A respectively [22; 23].

Following that same procedure, we estimated the free energy of noncovalent interactions involving the residues Q39 and E451 and OH4 (in the equatorial and axial positions) and OH6 of the substrate for the A263F and S337F mutants (Table 3). The A263F mutation, which is distant 25 Å from the active site, caused a significant decrease in $Q39\text{-}OH4_{equatorial}$ and $Q39\text{-}OH4_{axial}$ interactions (5.6 *k*J/mol and 3.1 *k*J/mol, respectively). The $E451\text{-}OH4_{equatorial}$ and $E451\text{-}OH4_{axial}$ interactions were also weakened by the A263F mutation (Table 3). The S337F mutation, also distant 25 Å from the active site, decreased the stability of the $Q39\text{-}OH4_{equatorial}$ and $Q39\text{-}OH4_{axial}$ interactions (3.3 *k*J/mol and 2.4 *k*J/mol, respectively). The same reductions were observed for the $E451\text{-}OH4_{equatorial}$ and $E451\text{-}OH4_{axial}$ interactions. Finally, A263F and S337F mutations did not significantly change interactions involving OH6 (Table 3). In brief, these data show that specific noncovalent interactions involved in transition state stabilization within the Sfβgly active site were changed as a consequence of remote mutations S337F and A263F.

Mutation A263F caused a larger change in the interactions involving $OH4_{equatorial}$ compared to $OH4_{axial}$, whereas mutation S337F similarly affected interactions with $OH4_{equatorial}$ and $OH4_{axial}$. Considering that $OH4_{equatorial}$ occurs in NPβglc, whereas $OH4_{axial}$ is present in

Table 1. Kinetic parameters for the substrate hydrolysis by the wild-type and mutant Sfβgly.

		kinetic parameter		
enzyme	**substrate**	K_m (mM)	k_{cat} (s^{-1})	k_{cat}/K_m
wild-type	*p*NPβGlu	0.87 ± 0.04	2.56 ± 0.02	2.9 ± 0.1
	*p*NPβFuc	0.81 ± 0.07	5.8 ± 0.2	7.1 ± 0.7
	*p*NPβGal	4.0 ± 0.2	0.322 ± 0.006	0.080 ± 0.004
	cellobiose	5.0 ± 0.6	2.14 ± 0.08	0.42 ± 0.05
D260A	*p*NPβGlu	1.05 ± 0.06	1.63 ± 0.03	1.5 ± 0.1
	*p*NPβFuc	0.82 ± 0.05	2.95 ± 0.09	3.6 ± 0.2
	*p*NPβGal	4.1 ± 0.3	0.223 ± 0.004	0.054 ± 0.004
	cellobiose	7 ± 1	1.45 ± 0.07	0.21 ± 0.03
E261A	*p*NPβGlu	0.94 ± 0.01	2.10 ±0.06	2.23 ± 0.07
	*p*NPβFuc	0.80 ± 0.06	5.3 ± 0.2	6.6 ± 0.5
	*p*NPβGal	3.6 ± 0.2	0.310 ± 0.006	0.086 ± 0.005
	cellobiose	4.5 ± 0.3	1.89 ± 0.04	0.42 ± 0.03
M262A	*p*NPβGlu	1.04 ± 0.07	2.64 ± 0.05	2.5 ± 0.2
	*p*NPβFuc	1.4 ± 0.1	7.9 ± 0.5	5.7 ± 0.5
	*p*NPβGal	3.2 ± 0.4	0.32 ± 0.01	0.10 ± 0.01
	cellobiose	4.5 ± 0.3	2.13 ± 0.04	0.47 ± 0.03
A263F	*p*NPβGlu	1.60 ± 0.06	0.806 ± 0.008	0.50 ± 0.05
	*p*NPβFuc	0.64 ± 0.06	1.35 ± 0.05	2.1 ± 0.2
	*p*NPβGal	5.2 ± 0.4	0.194 ± 0.007	0.037 ± 0.003
	cellobiose	6.8 ± 0.7	0.72 ± 0.04	0.11 ± 0.01
E265A	*p*NPβGlu	1.4 ± 0.1	1.86 ± 0.04	1.3 ± 0.1
	*p*NPβFuc	1.5 ± 0.1	6.4 ± 0.5	4.3 ± 0.4
	*p*NPβGal	4.5 ± 0.4	0.278 ± 0.008	0.062 ± 0.006
	cellobiose	7.8 ± 0.7	1.74 ± 0.07	0.22 ± 0.02
L335A	*p*NPβGlu	1.2 ± 0.1	1.57 ± 0.05	1.3 ± 0.1
	*p*NPβFuc	0.61 ± 0.05	3.4 ± 0.1	5.6 ± 0.5
	*p*NPβGal	3.7 ± 0.2	0.247 ± 0.005	0.067 ± 0.004
	cellobiose	5.8 ± 0.5	1.07 ± 0.03	0.18 ± 0.02
S337F	*p*NPβGlu	1.4 ± 0.1	0.96 ± 0.02	0.68 ± 0.05
	*p*NPβFuc	0.45 ± 0.02	1.24 ± 0.01	2.7 ± 0.1
	*p*NPβGal	5.7 ± 0.5	0.147 ± 0.005	0.026 ± 0.002
	cellobiose	7 ± 1	0.50 ± 0.03	0.07 ± 0.01
L389A	*p*NPβGlu	0.69 ± 0.06	0.76 ± 0.01	1.1 ± 0.1
	*p*NPβFuc	0.8 ± 0.1	2.1 ± 0.1	2.6 ± 0.3
	*p*NPβGal	3.2 ± 0.5	0.148 ± 0.007	0.046 ± 0.008
	cellobiose	nd	nd	nd
N391A	*p*NPβGlu	1.07 ± 0.06	1.22 ± 0.02	1.14 ± 0.07
	*p*NPβFuc	0.7 ± 0.1	2.8 ± 0.2	4.1 ± 0.6
	*p*NPβGal	4.5 ± 0.6	0.20 ± 0.01	0.044 ± 0.006
	cellobiose	nd	nd	nd

nd, not determined.

https://doi.org/10.1371/journal.pone.0198696.t001

NPβgal and NPβfuc, the preferential effect of the A263F mutation on interactions with $OH4_{equatorial}$ should cause a change in the substrate specificity, whereas the S337F mutation should have a less severe effect on the specificity. Actually, the k_{cat}/K_m ratio between NPβglc and

Table 2. Changes in the activation free energy ($\Delta\Delta G^{\ddagger}$) for substrate hydrolysis due to mutations of Sfβgly.

mutation	substrate	$\Delta\Delta G^{\ddagger}$ ($kJ.mol^{-1}$)
D260A	*p*NPβGlu	1.7 ± 0.1
	*p*NPβFuc	1.7 ± 0.2
	*p*NPβGal	0.99 ± 0.08
	cellobiose	1.7 ± 0.3
E261A	*p*NPβGlu	0.66 ± 0.03
	*p*NPβFuc	0.18 ± 0.02
	*p*NPβGal	- 0.18 ± 0.01
	cellobiose	0
M262A	*p*NPβGlu	0.37 ± 0.03
	*p*NPβFuc	-0.55 ± 0.07
	*p*NPβGal	- 0.56 ± 0.06
	cellobiose	– 0.28 ± 0.03
A263F	*p*NPβGlu	4.4 ±0.4
	*p*NPβFuc	3.1 ± 0.4
	*p*NPβGal	1.9 ± 0.2
	cellobiose	3.4 ± 0.5
E265A	*p*NPβGlu	2.0 ± 0.2
	*p*NPβFuc	1.2 ± 0.1
	*p*NPβGal	0.64 ± 0.07
	cellobiose	1.6 ± 0.2
L335A	*p*NPβGlu	2.0 ± 0.2
	*p*NPβFuc	0.60 ± 0.07
	*p*NPβGal	0.45 ± 0.03
	cellobiose	2.1 ± 0.3
S337F	*p*NPβGlu	3.6 ± 0.3
	*p*NPβFuc	2.4 ± 0.2
	*p*NPβGal	2.8 ± 0.2
	cellobiose	4.5 ± 0.8
L389A	*p*NPβGlu	2.4 ± 0.2
	*p*NPβFuc	2.5 ± 0.4
	*p*NPβGal	1.4 ± 0.2
	cellobiose	nd
N391A	*p*NPβGlu	2.3 ± 0.2
	*p*NPβFuc	1.4 ± 0.2
	*p*NPβGal	1.5 ± 0.2
	cellobiose	nd

Positive $\Delta\Delta G^{\ddagger}$ values corresponds to less stable $ES^{\ddagger}$ complex.
nd, not determined.

https://doi.org/10.1371/journal.pone.0198696.t002

NPβgal for the A263F mutant (14 ± 2) is about half of the ratio for the wild-type Sfβgly (36 ± 2), whereas the ratio for S337F (26 ± 3) is similar to the remaining mutants (20–28) and closer to the wild-type. Hence, A263F mutation really reduced the Sfβgly preference for NPβglc *versus* NPβgal.

Therefore only a subset of the studied mutations had an effect on the catalytic properties of the Sfβgly active site. Specifically, A264F and V336F drastically reduced the Sfβgly activity, while A263F and S337F only weakened the interactions that stabilize the transition state.

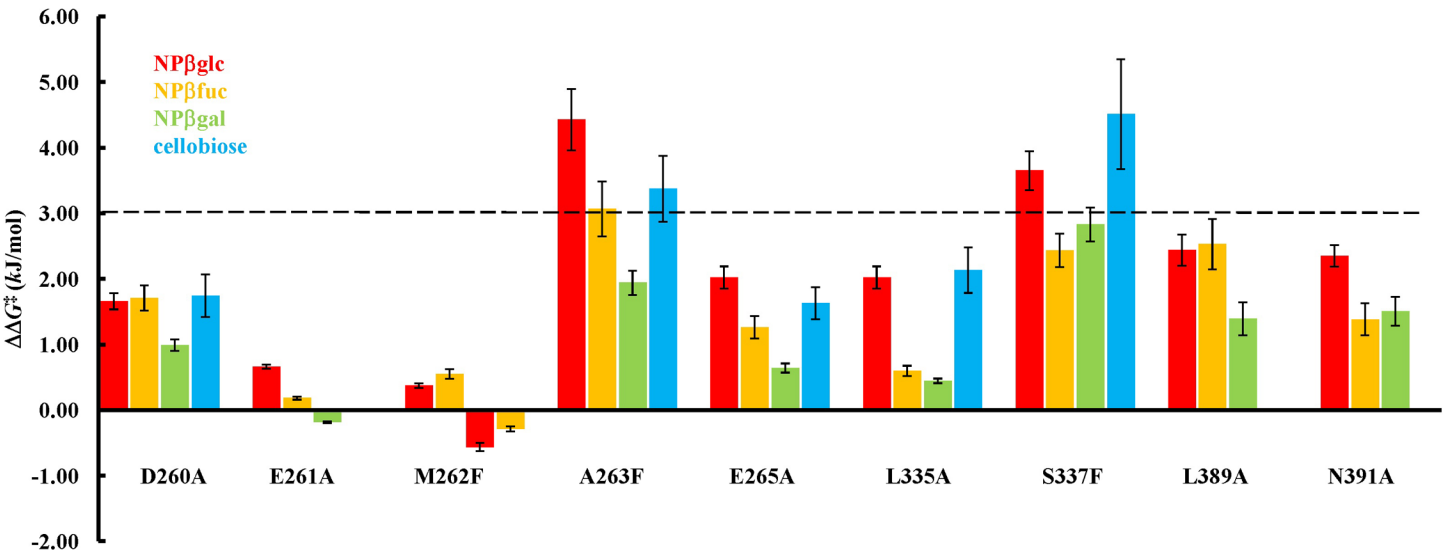

Fig 2. Mutational effects on the stability of the ES‡ complexes involving different substrates. $\Delta\Delta G^{\ddagger}$ were determined based on the k_{cat}/K_m for the hydrolysis of different substrates. See the Materials and Methods for more details.

https://doi.org/10.1371/journal.pone.0198696.g002

Remarkably, side chains of A263 and A264 project from the α-helix lateral towards F251, whereas E261, M262 and E265, sites of innocuous mutations, are in the opposite side of the α-helix (Fig 1A). D260, even projecting its side chain from the same α-helix side as A263 and A264, is far from F251 by about 10 Å. Similarly, V336 and S337,which also affected catalysis, are part of a β-strand close to F251 (Fig 1A). In fact, the side chain of V336 is pointed directly at F251. The different outcomes of mutations placed in the same structural element suggest that the relative position of mutated residues to hub F251 is important.

A similar relationship between the spatial distribution of this same set of mutations was also observed in the analysis of the thermal stability of Sfβgly [25]. Indeed, mutational effects on the relative melting temperature (T_m) and relative k_{cat}/K_m are similar (correlation coefficient = 0.85; Fig 3), suggesting that changes in Sfβgly thermal stability and catalysis may arise from the same structural pertubations.

Residues A263, A264, V336 and S337 are closely packed, forming an internal region between the α-helix and the β-strand in which F251 is also inserted (Fig 1B). The relative

Table 3. Free energy estimated for noncovalent interactions involving active site residues Q39 and E451 and glycone hydroxyls 4 and 6 in the ES‡ complex of the wild-type and mutant Sfβgly.

	Enzyme		
	wild-type	A263F	S337F
Interaction		$\Delta G^{\ddagger}$ ($kJ.mol^{-1}$)	
Q39-OH4$_{equatorial}$	21.9	16.3	18.6
Q39-OH4$_{axial}$	14.3	11.3	11.9
Q39-OH6	1.3	2.4	0.9
E451-OH4$_{equatorial}$	35.7	30.2	32.5
E451-OH4$_{axial}$	18.9	15.8	16.5
E451-OH6	-6.5	-5.3	-6.8

The $\Delta G^{\ddagger}$ were calculated considering the disruption of the interaction. Hence positive values corresponds to an interaction that stabilize the ES‡ complex, whereas a negative value indicates the opposite effect.

https://doi.org/10.1371/journal.pone.0198696.t003

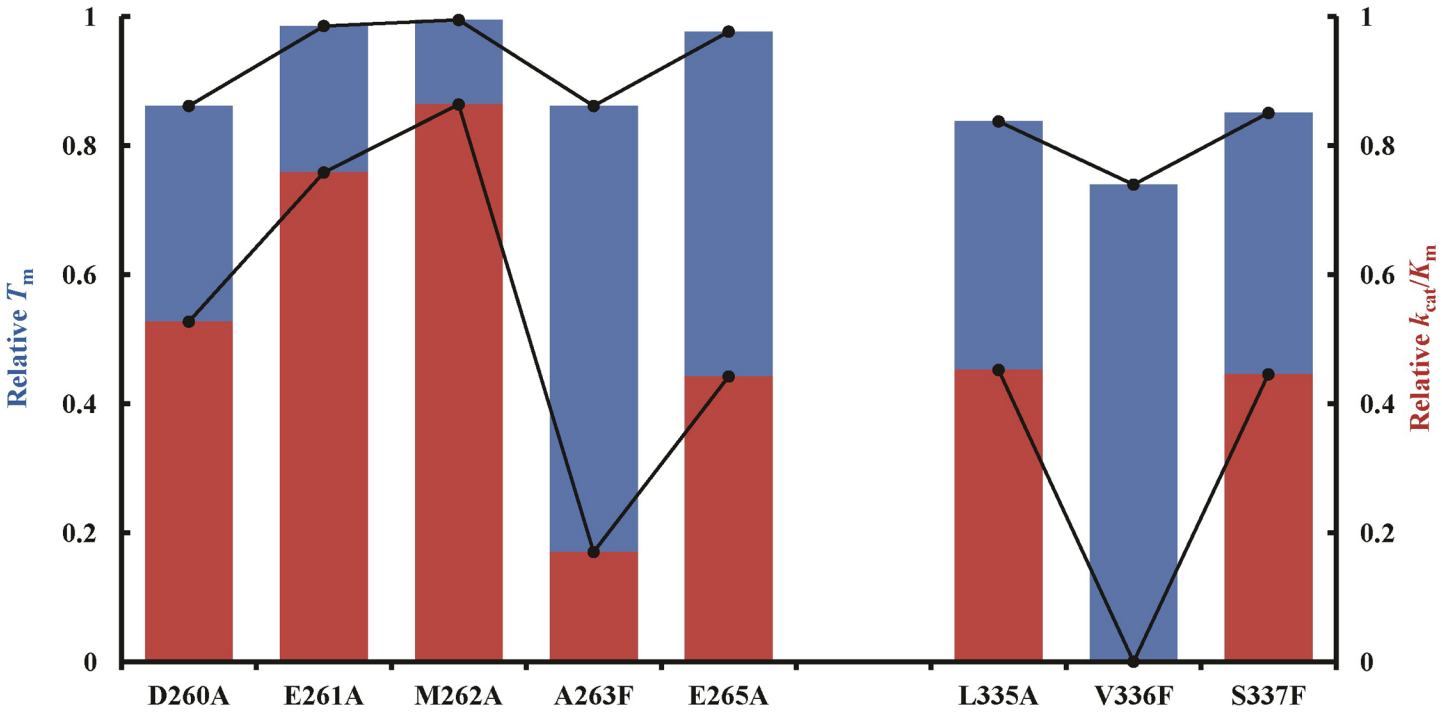

Fig 3. Effect of the mutations on the thermal stability (blue) and enzyme activity (red) of Sfβgly. Melting temperatures (T_m) were obtained in [25]. The A264F mutant was not included because it unfolds through a multiple intermediate pathway. Hence it does not present a single T_m [25]. k_{cat}/K_m are from Table 1. Lines were added to make it easier to follow the trends. The correlation coefficient between the Relative T_m and Relative k_{cat}/K_m is 0.85.

https://doi.org/10.1371/journal.pone.0198696.g003

solvent accessible area of these residues ranges from 0 to 10%. Therefore, replacement of the residues A263, A264, V336 and S337 by phenylalanine possibly perturbed their packing and altered the spatial positioning and conformation of residue F251.

Due to the high centrality of F251 in the Sfβgly PSN, we speculate that spatial perturbations on this residue could effectively spread and reach the active site. In detail, F251 directly contacts N249 and F334, which interacts with Y331 and W371. The side chain of W371 interacts with the substrate aglycone [17; 21], whereas Y331 contacts the catalytic nucleophile E399 and W444, which binds the glycone substrate [20; 31]. Hence, two contacts were supposedly enough to link F251 to the active site residues involved in substrate binding and catalysis. Although it is still speculative to determine details of the structural perturbations involved in the mutants, we suggest that the high centrality of F251 increased the chance that perturbations directed to it resulted in structural alterations of the active site.

Conclusion

Mutations A263F, A264F, V336F and S337F may directly perturb the position and conformation of hub F251, which could effectively propagate these perturbations into the Sfβgly active site through short connection pathways along the protein network. This is an indication that analysis of a PSN could be valuable to predict the outcome of mutations on enzymatic activity and other protein functions.

Supporting information

S1 Fig. Kinetic scheme of the reaction catalyzed by GH1 β-glucosidases. Substrate S is formed by a monosaccharide (glycone; G) covalently linked to a group called aglycone (Ag).

After the glycosidic bond cleavage, step 2, a glycosyl-enzyme intermediate (E-G) is formed and the first product, Ag, is released. In the step 3, the intermediate is hydrolyzed releasing the second product, G. Based on [19; 29].
(TIFF)

S2 Fig. Effect of the concentration on the initial rate of substrate hydrolysis catalyzed by the wild-type and mutant Sfβgly. NPβglc, *p*-nitrophenyl β-glucoside; NPβgal, *p*-nitrophenyl β-galactoside; NPβfuc, *p*-nitrophenyl β-fucoside) and cellobiose. The mutants are identified in each panel. Lines represent the best fit of the data to the Michaelis-Menten equation. The substrates were prepared in 50 mM sodium citrate–sodium phosphate buffer at pH 6.
(TIFF)

S3 Fig. The active site of Sfβgly. E399 is the catalytic nucleophile. Noncovalent interactions with the residues R97 and Y331 modulate ionization of E399. The residues Q39, H142 and E451 bind the substrate glycone (glc; 2-deoxy-2-fluoro-β-D-glucose). The noncovalent contact distances are: $E399_{O\varepsilon}$ –$R97_{N\eta}$, 3.6 Å; $E399_{O\varepsilon}$ –$Y331_{O\eta}$, 2.7 Å; $E451_{O\varepsilon}$ –OH4, 2.2 Å; $E451_{O\varepsilon}$ –OH6, 2.7 Å; $Q39_{N\varepsilon2}$ –OH4, 2.7 Å; $Q39_{O\varepsilon1}$-OH3, 2.4 Å; $H142_{N\varepsilon2}$ –OH2, 3.0 Å. Contacts are indicated by yellow dashed lines. OH4, glycone hydroxyl 4; OH6, glycone hydroxyl 6. The active site interaction with the substrate glycone was based on the superposition of the crystallographic structures 5CG0 [17] and 1E70 [33].
(TIFF)

S1 Table. Hub residues of the Sfβgly protein structure network. The central residues, also termed hub residues, of the Sfβgly PSN were identified based on the effect of their removal on the network path length (*L*). The z-score indicated the normalized increase of *L* due to the residue removal. Thus, z-scores are expressed in terms of standard deviations (σ). Cells marked in red indicate residues that are part of the Sfβgly active site. This table is based on reference [25].
(DOCX)

Acknowledgments

S.R.M. and G.M.A. are staff members of the "Departamento de Bioquímica–IQUSP" and CNPq Research Fellows. V.P.S. and C.M.I. are graduate students supported by Fapesp and Capes, respectively. We thank Juliana Raveli Domingos for providing technical assistance.

Author Contributions

Conceptualization: Sandro R. Marana.

Formal analysis: Valquiria P. Souza, Cecília M. Ikegami, Guilherme M. Arantes, Sandro R. Marana.

Funding acquisition: Guilherme M. Arantes, Sandro R. Marana.

Investigation: Valquiria P. Souza, Cecília M. Ikegami, Guilherme M. Arantes, Sandro R. Marana.

Resources: Guilherme M. Arantes, Sandro R. Marana.

Writing – original draft: Valquiria P. Souza, Sandro R. Marana.

Writing – review & editing: Valquiria P. Souza, Guilherme M. Arantes, Sandro R. Marana.

References

1. Szalay KZ, Csermely P. Perturbation centrality and turbine: a novel centrality measure obtained using a versatile network dynamics tool. PLOS ONE 2013; 8(10): e78059. https://doi.org/10.1371/journal.pone.0078059 PMID: 24205090
2. Greene LH, Higman VA. Uncovering network systems within protein structures. J. Mol Biol. 2003; 334, 781–791. PMID: 14636602
3. Bagler G, Sinha S. Network properties of protein structures. Physica A-Stat Mech Appl. 2005; 346: 27–33.
4. Kundu S. Amino acid network within protein. Physica A-Stat Mech Appl. 2005; 346: 104–109.
5. Aftabuddin M, Kundu S. Hydrophobic, hydrophilic, and charged amino acid networks within protein. Biophys J. 2007; 93: 225–231. https://doi.org/10.1529/biophysj.106.098004 PMID: 17172302
6. del Sol A, O'Meara P. Small-world network approach to identify key residues in protein-protein interaction. Prot Struct Func Bioinfo. 2005; 58: 672–682.
7. Watts DJ, Strogatz SH. Collective dynamics of 'small-world' networks. Nature. 1998; 393: 440–442. https://doi.org/10.1038/30918 PMID: 9623998
8. Amitai G, Shemesh A, Sitbon E, Shklar M, Netanely D, Venger I et al. Network analysis of protein structures identifies functional residues. J Mol Biol 2004; 344: 1135–1146. https://doi.org/10.1016/j.jmb.2004.10.055 PMID: 15544817
9. Süel GM, Lockless SW, Wall MA, Ranganathan R. Evolutionarily conserved networks of residues mediate allosteric communication in proteins. Nature Struct Biol. 2003; 10: 59–69. https://doi.org/10.1038/nsb881 PMID: 12483203
10. Amaro RE, Sethi A, Myers RS, Jo Davisson V, Lythey-Schulten ZA. A network of conserved interactions regulates the allosteric signal in a glutamine amidotransferase. Biochem. 2007; 46: 2156–2173.
11. Goodey NM, Benkovic SJ. Allosteric regulation and catalysis emerge via a common route. Nature Chem Biol. 2008; 4: 474–482.
12. del Sol A, Tsai C-J, Ma B, Nussinov R. The Origin of Allosteric Functional Modulation: Multiple Pre-existing Pathways. Structure. 2009; 17: 1042–1050. https://doi.org/10.1016/j.str.2009.06.008 PMID: 19679084
13. Park K, Kim D. Modeling allosteric signal propagation using protein structure networks. BMC Bioinfo. 2011; 12: (Suppl 1) S23. https://doi.org/10.1186/1471-2105-12-S1-S23 PMID: 21342553
14. Doshi U, Holliday MJ, Eisenmesser EZ, Hamelberg D. Dynamical network of residue-residue contacts reveals coupled allosteric effects in recognition, catalysis, and mutation. PNAS. 2016; 113: 4735–4740. https://doi.org/10.1073/pnas.1523573113 PMID: 27071107
15. Halabi N, Rivoire O, Leibler S, Ranganathan R. Protein sectors: Evolutionary units of three-dimensional structure. Cell. 2016; 138: 774–786.
16. Richard J, Kim ED, Nguyen H, Kim CD, Kim S. Allostery wiring map for kinesin energy transduction and its evolution. J Biol Chem. 2016; 291: 20932–20945. https://doi.org/10.1074/jbc.M116.733675 PMID: 27507814
17. Tamaki FK, Souza DP, Souza VP, Ikegami CM, Farah CS, Marana SR. Using the Amino Acid Network to Modulate the Hydrolytic Activity of β-Glycosidases. PLOS ONE. 2016; 11(12): e0167978. https://doi.org/10.1371/journal.pone.0167978 PMID: 27936116
18. Marana SR, Jacobs-Lorena M, Terra WR, Ferreira C. Amino acid residues involved in substrate binding and catalysis in an insect digestive β-glycosidase. Biochim Biophys Acta -Prot Struct Mol Enzymol. 2001; 1545: 41–52.
19. Kempton JB, Withers SG. Mechanism of *Agrobacterium* β-glucosidase: kinetic studies. Biochem. 1992; 31: 9961–9969.
20. Marana SR, Mendonca LMF, Andrade EHP, Terra WR, Ferreira C. The role of residues R97 and Y331 in modulating the pH optimum of an insect β-glycosidase of family 1. Eur J Biochem. 2003; 270: 4866–4875. PMID: 14653813
21. Mendonça LMF, Marana SR. The role in the substrate specificity and catalysis of residues forming the substrate aglycone-binding site of a β-glycosidase. FEBS J. 2008; 275: 2536–2547. https://doi.org/10.1111/j.1742-4658.2008.06402.x PMID: 18422657
22. Marana SR, Terra WR, Ferreira C. The role of amino-acid residues Q39 and E451 in the determination of substrate specificity of the *Spodoptera frugiperda* β-glycosidase. Eur J Biochem. 2002; 269: 3705–3714. PMID: 12153567
23. Marana SR, Andrade EHP, Ferreira C, Terra WR. Investigation of the substrate specificity of a β-glycosidase from *Spodoptera frugiperda* using site-directed mutagenesis and bioenergetic analysis. Eur J Biochem. 2004; 271: 4169–4177. https://doi.org/10.1111/j.1432-1033.2004.04354.x PMID: 15511222

24. Badieyan S, Bevan DR, Zhang C. Probing the active site chemistry of β-glucosidases along the hydrolysis reaction pathway. Biochem. 2012; 51: 8907–8918.

25. Souza VP, Ikegami CM, Arantes GM, Marana SR. Protein thermal denaturation is modulated by central residues in the protein structure network. FEBS J. 2016; 283: 1124–1138. https://doi.org/10.1111/febs.13659 PMID: 26785700

26. Gill SC, von Hippel PH. Calculation of proteins extinction coefficients from amino acid sequence data. Anal Biochem. 1989; 182: 319–326. PMID: 2610349

27. Gasteiger E, Hoogland C, Gattiker A, Duvaud S, Wilkins MR, Appel RD, et al. *Protein Identification and Analysis Tools on the ExPASy Server*. In: Walker JM editor. The Proteomics Protocols Handbook. Humana Press; 2005. pp. 571–607.

28. Fersht A. Structure and mechanism in protein science: a guide to enzyme catalysis and protein folding, W.H. Freeman; 1999.

29. Namchuk M, Withers SG. Mechanism of *Agrobacterium* β-glucosidase: Kinetic analysis of the role of noncovalent enzyme/substrate interactions. Biochem. 1995; 34: 16194–16202.

30. Fersht A, Shi J-P, Knill-Jones J, Lowe DM, Wilkinson AJ, Blow DM et al. Hydrogen bonding and biological specificity analysed by protein engineering. Nature. 1985; 314: 235–238. PMID: 3845322

31. Marana SR. Molecular Basis of Substrate Specificity in Family 1 Glycoside Hydrolases. IUBMB Life. 2006; 58: 67–73.

32. Cairns JRK, Esen A. β-glucosidases. Cell Mol Life Sci. 2010; 67: 3389–3405. https://doi.org/10.1007/s00018-010-0399-2 PMID: 20490603

33. Burmeister WP, Cottaz S, Rollin P, Vasella A, Henrissat B. High resolution X-ray crystallography shows that ascorbate is a cofactor for myrosinase and substitutes for the function of the catalytic base. J Biol Chem. 2000; 275: 39385–39393. https://doi.org/10.1074/jbc.M006796200 PMID: 10978344